

Attachment holding figures and tables to Final Report Summary – InnoREX



Project logo

Partner	Role within Project/ Competences	Contact
<i>Fraunhofer ICT</i>	Coordination of the project Online analytics: NIR Combining all elements to InnoREX production line Process realisation	Björn Bergmann Phone +49 721 4640-423 bjoern.bergmann@ict.fraunhofer.de
<i>Gneuss GmbH</i>	Online viscometry MRS degassing extruder Filtration Systems Measurement technology	Alexander Frank Phone + 49 5731 5307 122 alexander.frank@gneuss.de
<i>University of Mons</i>	Catalyst development Reaction kinetics	Jean-Marie Raquez Phone +32 65 37 34 81 jean-marie.raquez@umons.ac.be
<i>Hielscher Ultrasonics GmbH</i>	Ultrasound incorporation	Thomas Hielscher Phone +49 33 28 43 73 thomas@hielscher.com
<i>Muegge GmbH</i>	Microwave incorporation	Joachim Schneider Phone +49 6164-9307-66 joachim.schneider@muegge.de
<i>Sciences & Computers Consultants Sarl</i>	Enhancing Ludovic software	Chantal David Phone +33 4 77 49 75 82 scc@scconsultants.com
<i>Materia Nova</i>	Life Cycle Analysis	Olivier Talon Phone +32 65 55 49 18 olivier.talon@materianova.be
<i>BH Industries</i>	Upscaling strategy	Marian Soja Phone +48 69 39 31417 m.soja@bhproject.pl
<i>Talleres Pohuer SL</i>	Injection moulding	Pablo Querol Phone +34 96 555 09 35 investigacion@pohuer.es
<i>Asociacion de investigacion de materiales plasticos y conexas – AIMPLAS</i>	Additivition strategy Sheet extrusion	Carolina Losada Phone +34 961 366 040 closada@aimplas.es
<i>Associazione nazionale costruttori di macchine e stampi per materie plastiche e gomma - ASSOCOMAPLAST</i>	Dissemination and Exploitation	Girolamo Dagostino Phone +39 028 228 37 54 g.dagostino@assocomoplast.org
<i>Cranfield University</i>	Modelling of reaction kinetics in extrusion conditions	Hrushikesh Abhyankar Phone +44 1234758085 h.a.abhyankar@cranfield.ac.uk

List of beneficiaries and contact names

Description of the main S&T results / foregrounds

University of Mons: Catalyst development for the bulk polymerization of *L*-lactide

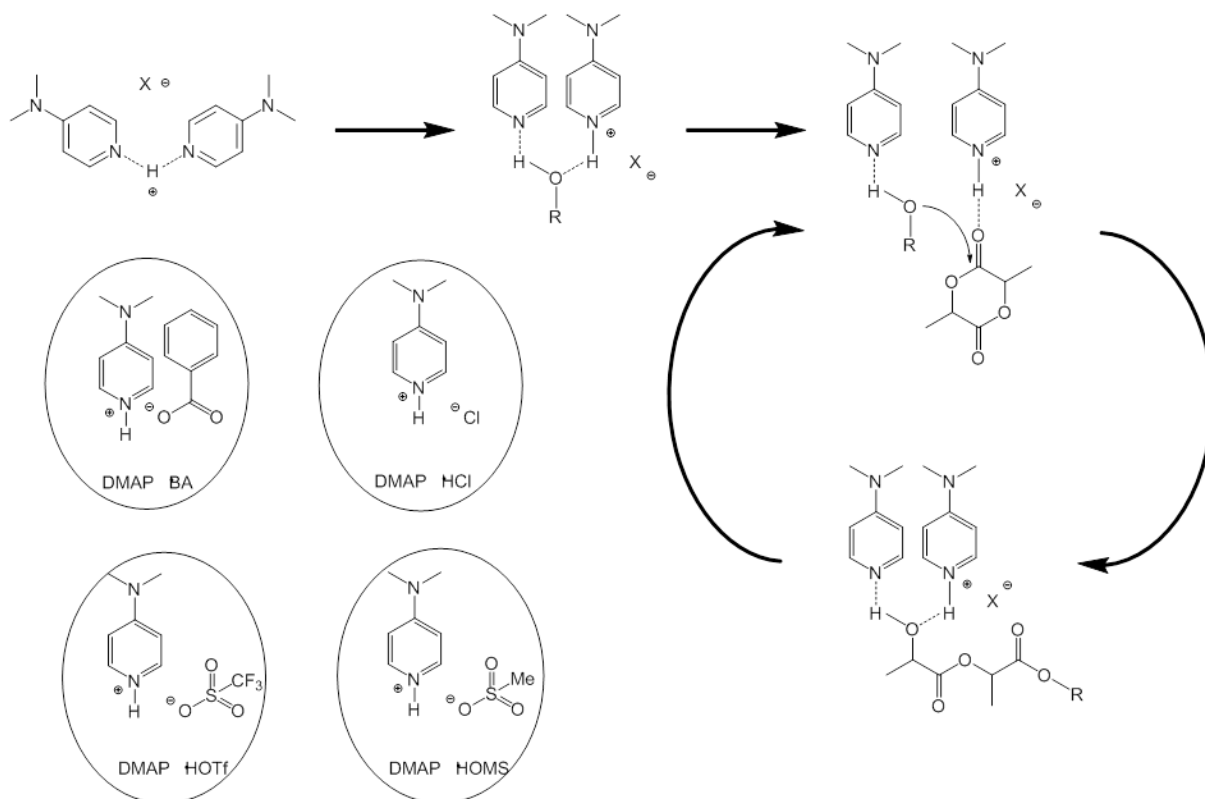


Figure 1: Proposed mechanism for DMAP/DMAP.HX catalyzed ROP of lactide (X is benzoate, chloride, trifluoromethane sulphonate, methane sulphonate)

a) DBU Conjugate salt

b) Betaine(s)

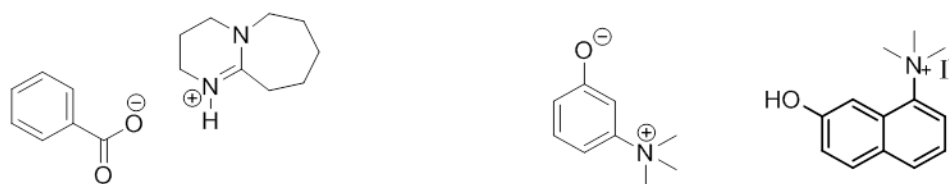


Figure 2: Examples of organic catalysts a) DBU benzoate conjugate salt and b) (trimethylammonio)-phenolate betaine and (7-Hydroxylate-naphthalen-2-yl)-trimethyl-ammonium

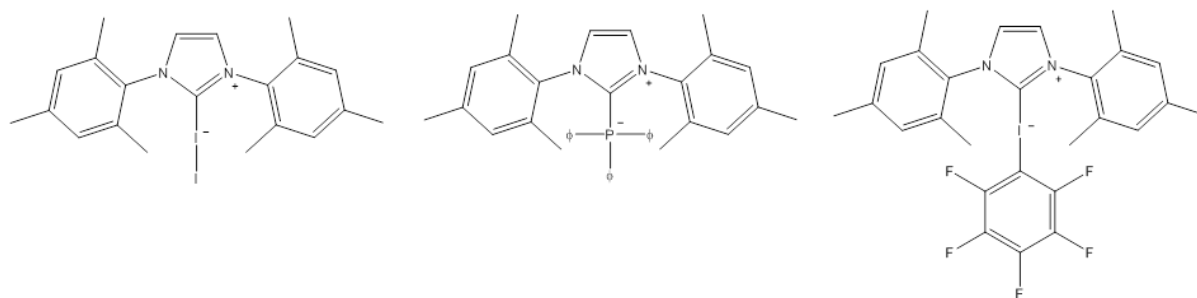


Figure 3: Examples of 5-membered carbene catalysts

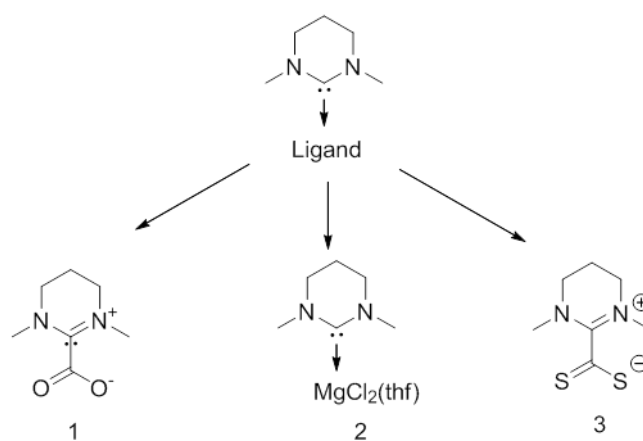


Figure 4: 6-membered N-heterocycle carbenes 1) 1,3-dimethyl-3,4,5,6-tetra- hydroypyrimidin-1-ium-2- carboxylate 2) 1,3-dimethyl-3,4,5,6-tetrahydro pyrimidin-1-ium-2-MgCl₂ (Mg-NHC) 3) 1,3-dimethyl-3,4,5,6- tetrahydroypyrimidin-1-ium-2-carbodithioate

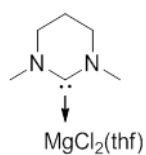


Figure 5: 1,3-dimethyl-3,4,5,6-tetrahydroypyrimidin-1-ium-2-MgCl₂ (Mg-NHC)

Table 1: Characterization data for P(L-LA) obtained by carbene-MgCl₂ (six-membered ring NH) catalyst polymerization at 170°C & 190°C.

Temperature (°C)	Time (min)	Conversion by ¹ H NMR ^b (%)	<i>M_n</i> ^a (g/mol)	[catalyst] ^o / [initiator] ^o / [monomer]	<i>M_p</i> ^a (g/mol)	<i>D_M</i> ^a
170	5	64	39,000	1/0/400	63,000	1.61
190		72	33,000		61,000	1.73
170	15	76	38,000	1/0/400	64,000	1.70
190		80	27,000		56,000	1.95
170	30	80	41,000	1/0/400	66,000	1.66
190		90	24,000		50,000	2.01
170	45	83	35,000	1/0/400	66,000	1.88
190		92	19,500		49,000	2.3
170	60	85	33,000	1/0/400	66,000	1.94
190		95	18,300		35,700	2.14

^a by GPC in CHCl₃, PS standards, 1 ml.min⁻¹, T = 30°C, ^b by 500MHz ¹H NMR

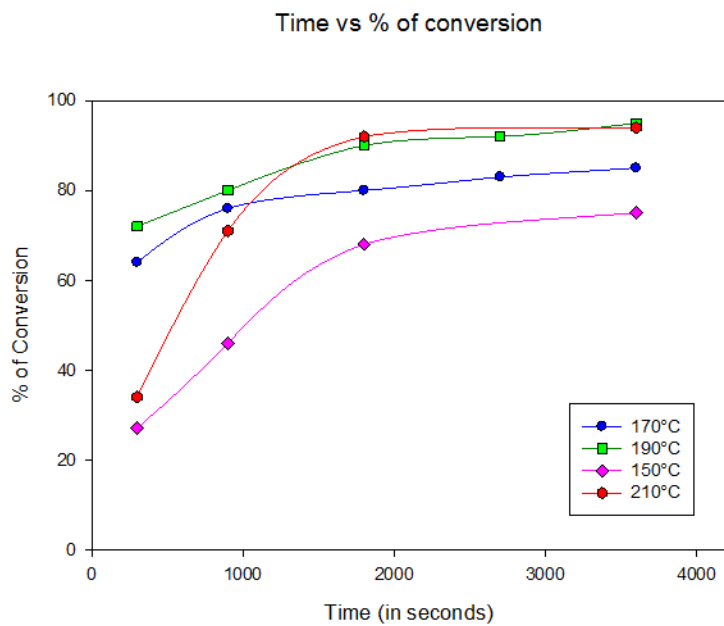


Figure 6: Kinetics of Mg-NHC ROP of L-Lactide without solvent and initiator (alcohol)

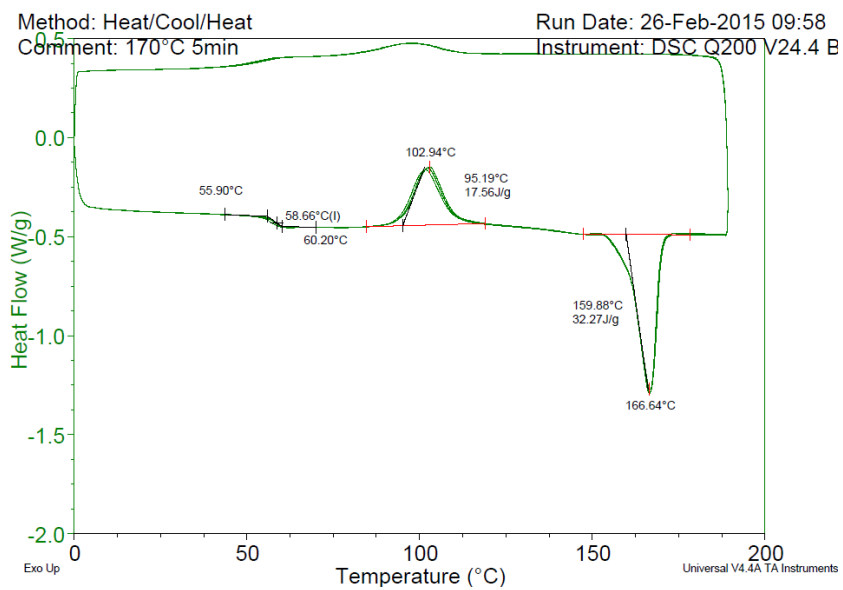


Figure 7: Five-cycle DSC analyses of high molecular weight PLA obtained at 170°C (see Table 1) – from 0 to 190°C at both heating/cooling rates of 10°C/min).

Table 2: Evolution of the extrusion force recorded during the extrusion synthesis of PLA (170°C – 75 RPM).

Time (min)	Force (N)
3*	30
6	40
7	50
8.5	75
9	80
10	85
11	93
12	98
13	100
14	103
15	105
16	108
18	110

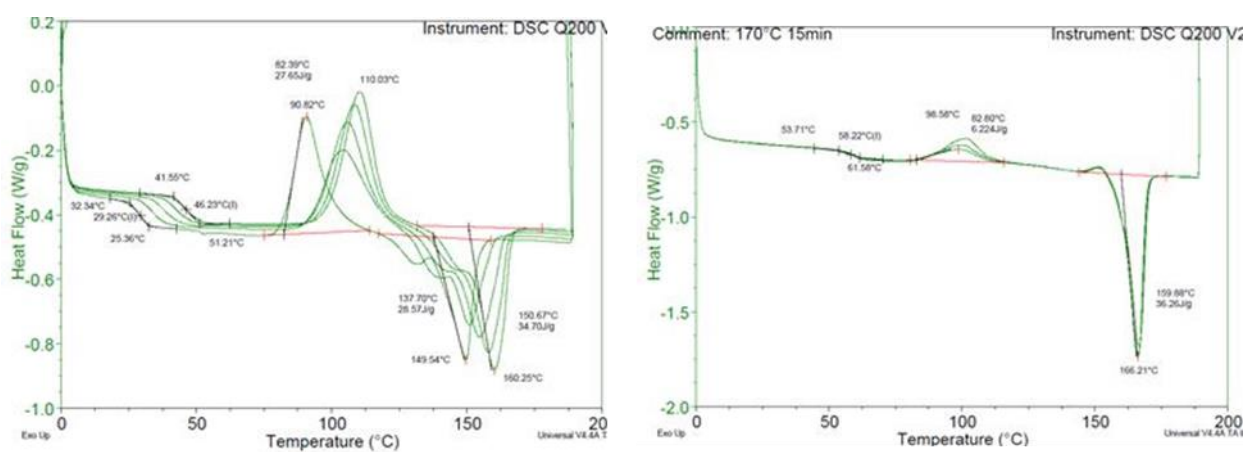


Figure 8: Five-cycle DSC analyses carried out on high molecular weight PLA obtained by extrusion before (a) and after monomer purification (b) (see Table 2 – from 0 to 190°C at both heating/cooling rates of 10°C/min).

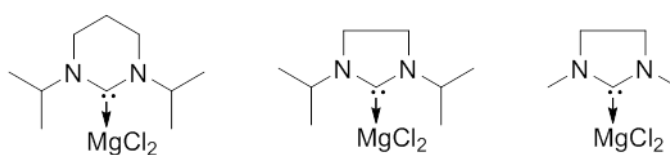


Figure 9: Variation in Mg-NHC

Hielscher: Ultrasonic Polymerization



Figure 10: Ultrasonic lab device UP200St for preliminary tests in smaller scale

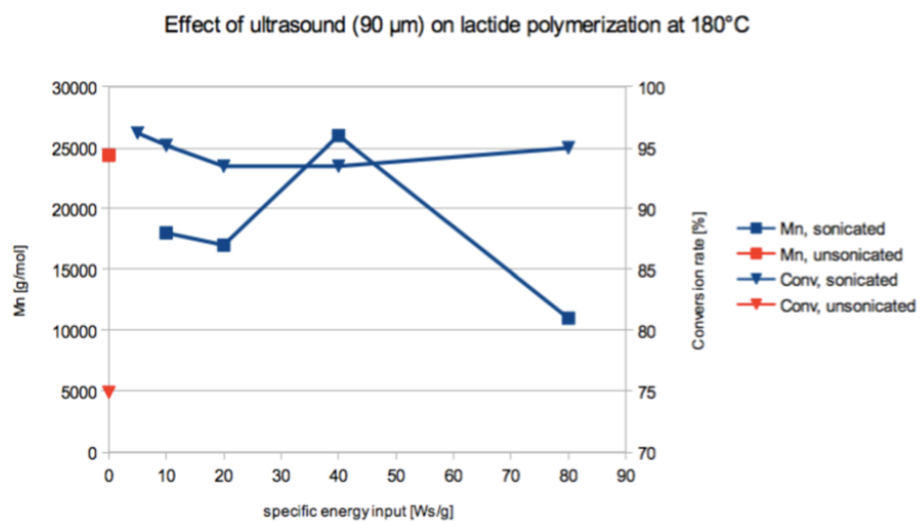


Figure 11: Effects of sonication (90 μm) on lactide polymerization at 180°C



Figure 12: Setup - Ultrasonic batch reactor with pressure sensor and temperature sensor



Figure 13: MPC48 with 48 cannulas for fine-size pre-mixing under sonication

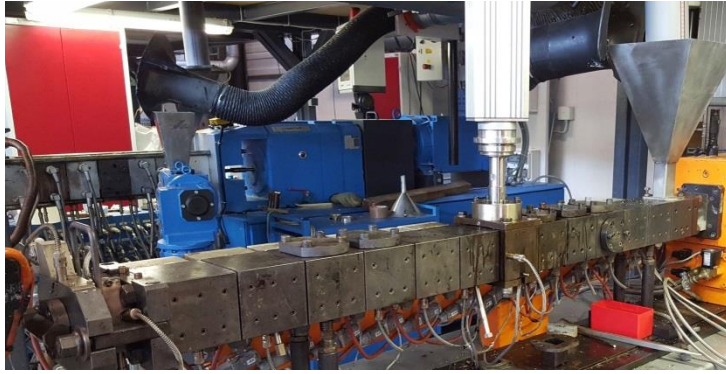


Figure 14: UIP2000hdT on extruder



Figure 15: Extruder block for the integration of the ultrasonic device into the twin screw extruder



Figure 16: Reactor for post-extrusion sonication

MUEGGE: Development, design and setup of an extruder block for injection of microwave energy

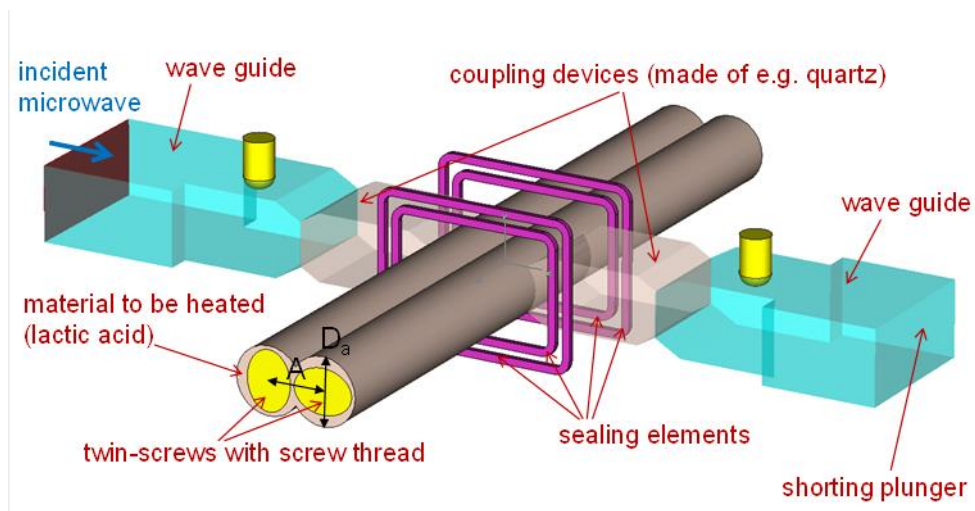


Figure 17: CAD model for coupling of 5.8 GHz microwave to the lab-scale twin screw extruder

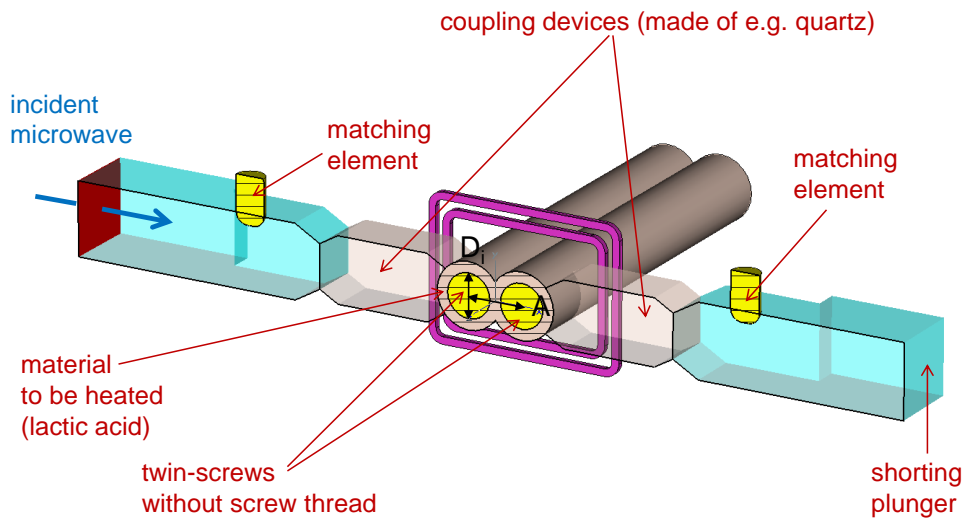


Figure 18: Vertical cross-section alongside the plane spanned by the cylindrical axes of the two matching elements. The diameter of each twin screw without screw thread is $D_i = 12$ mm, and the distance between the centers of the two screws is $A = 15$ mm

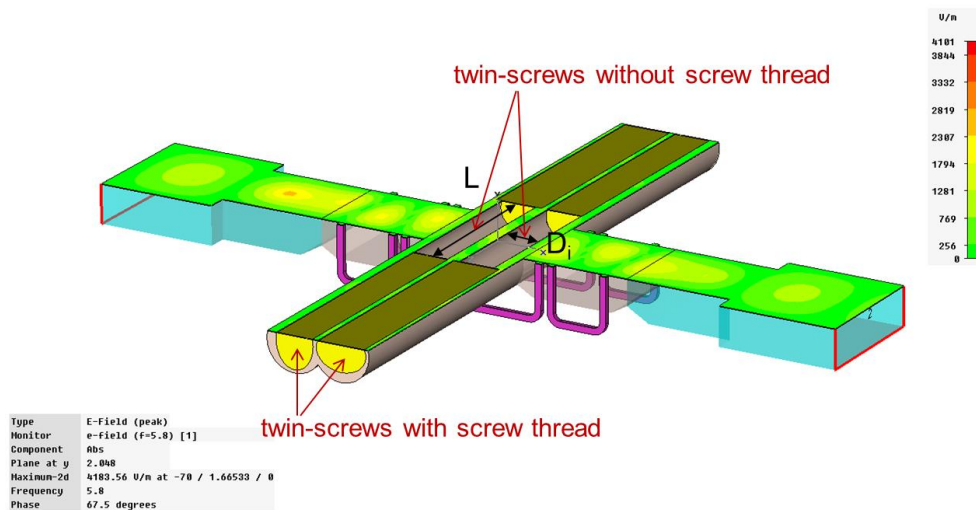


Figure 19: Distribution of the electrical field strength in the horizontal plane

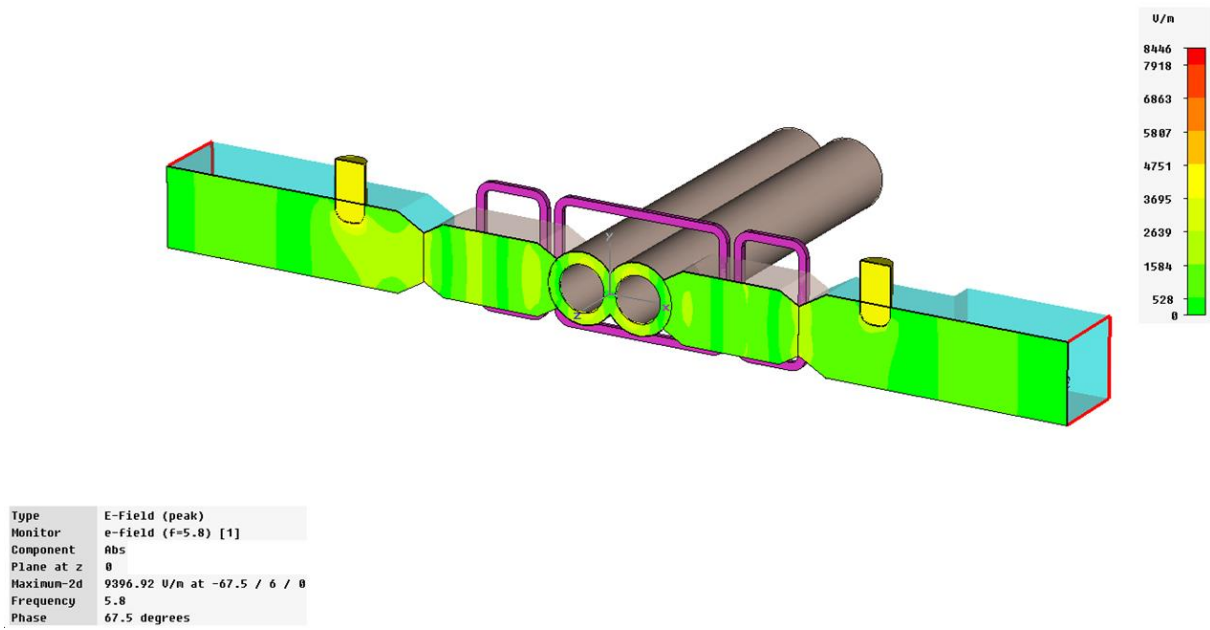


Figure 20: Distribution of the electrical field strength in the vertical plane

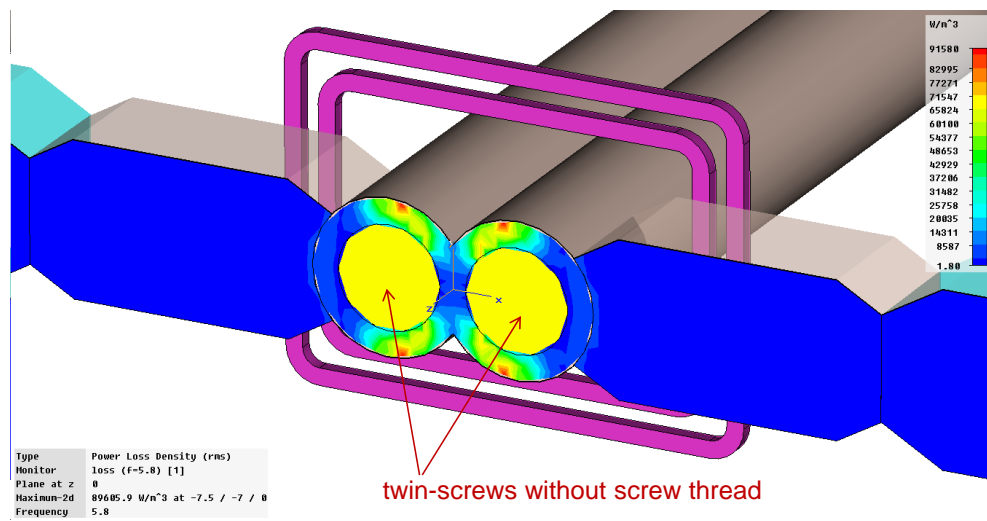


Figure 21: Distribution of the power density in the vertical plane corresponding to the vertical cross-section alongside the plane spanned by the cylindrical axes of the two matching elements

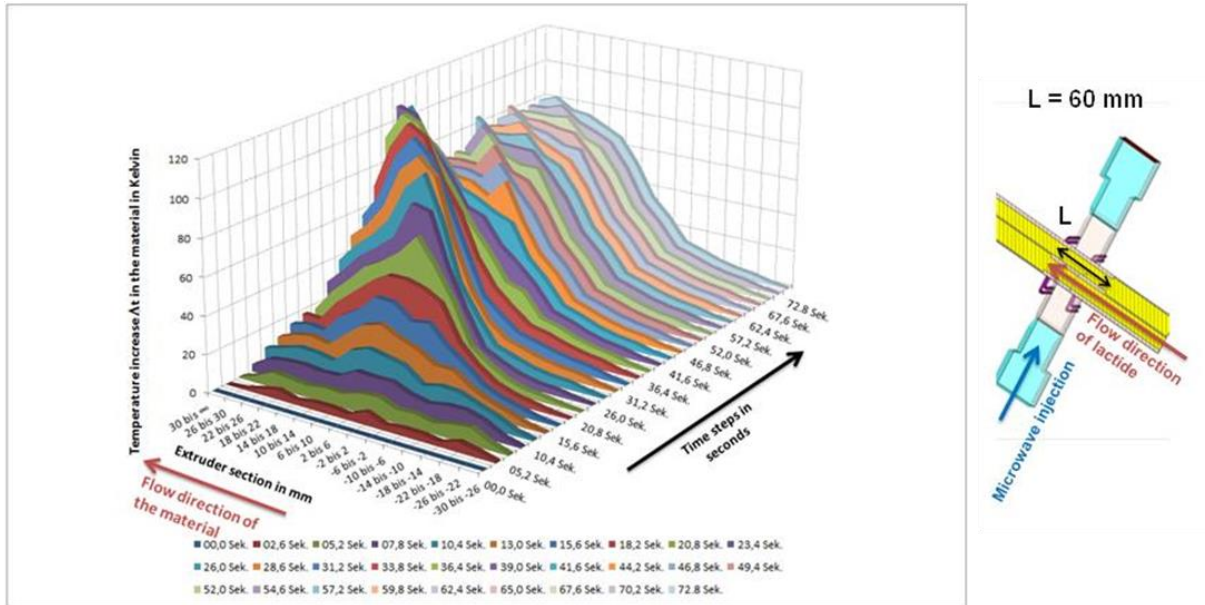


Figure 22: Time-related temperature profiles of the lactic acid in the extruder block for microwave injection

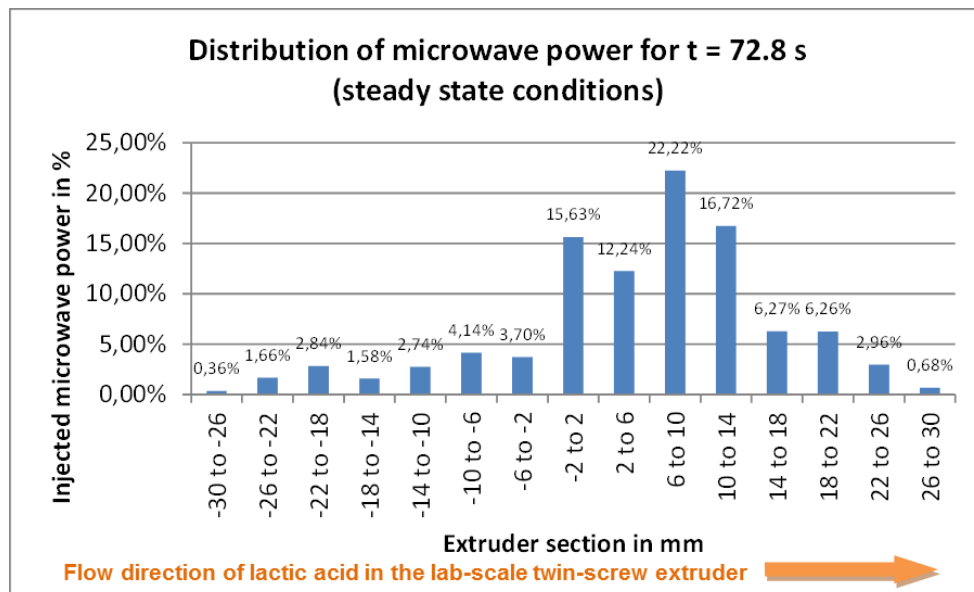


Figure 23: Results obtained from the simulations for the distribution of the microwave power in the different sections of the extruder block for injection of the 5.8 GHz microwave into the lab-scale twin screw extruder at Fraunhofer ICT at steady state conditions



Figure 24: Extruder block designed for microwave injection into the lab-scale twin screw extruder, connected to the shorting plunger on the right and to the E/H tuner on the left (only partly visible) of the 5.8 GHz microwave injection line



Figure 25: 5.8 GHz microwave injection line including (from left to right) a short piece of R 58 rectangular waveguide, an E/H tuner, the extruder block designed for microwave injection into the lab-scale twin screw extruder, and a shorting plunger

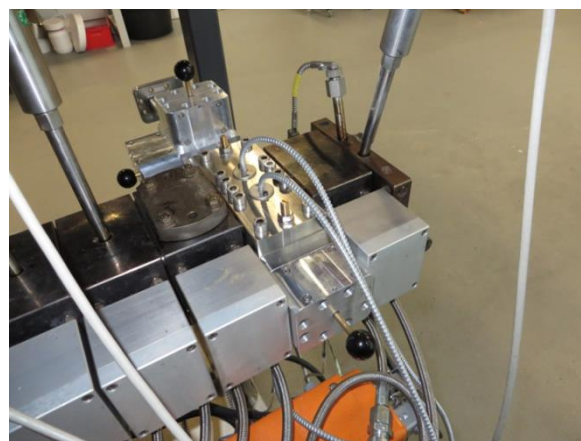


Figure 26: 5.8 GHz microwave injection line including a short R 58 rectangular waveguide, an E/H tuner, the extruder block and a shorting plunger, integrated into the lab-scale twin screw extruder at Fraunhofer ICT

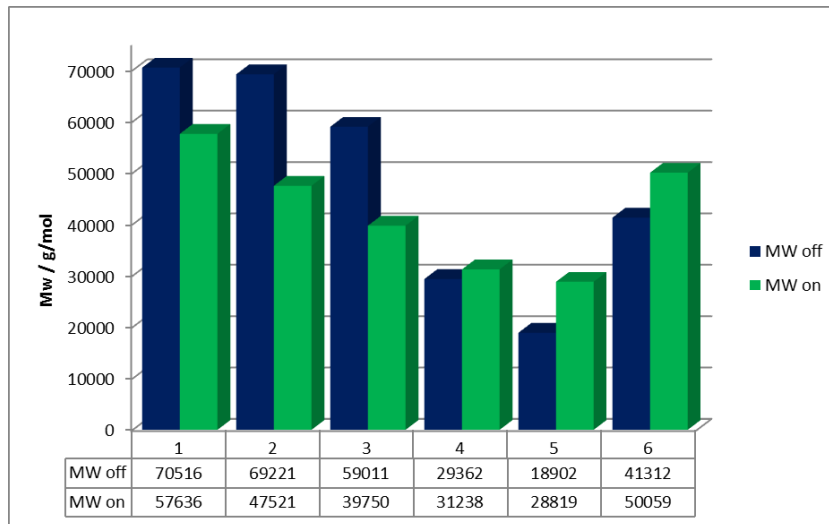


Figure 27: Molecular weight of the resulting PLA obtained for different process settings, with and without application of additional microwave energy injection

Gneuss: Degassing extruder and online viscometer development

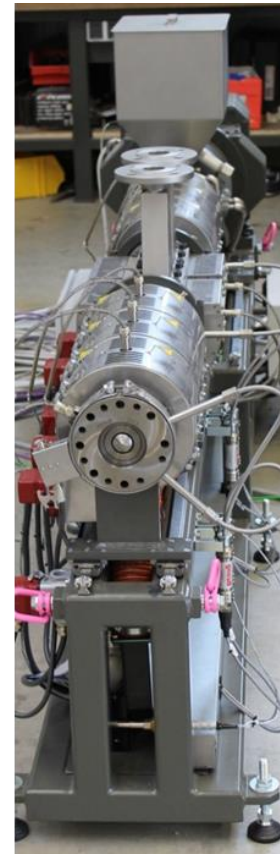
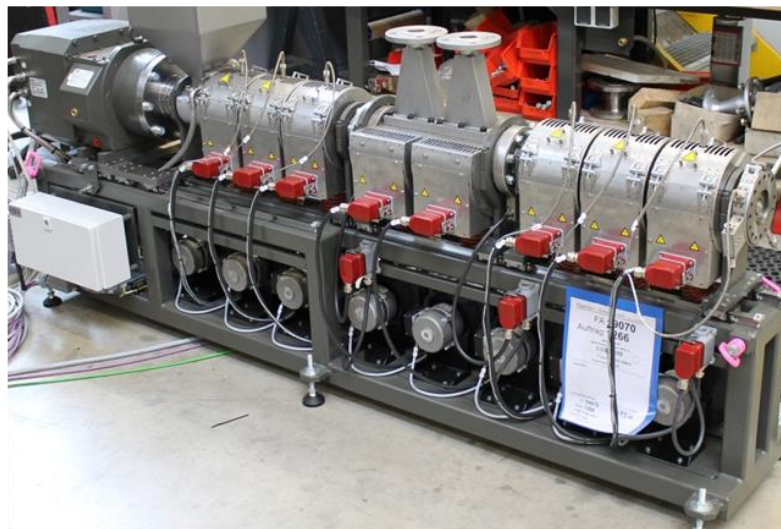
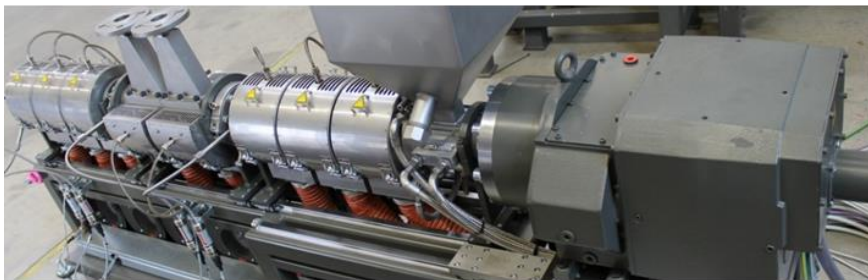


Figure 28: Prototype of MRS lab size extrusion system built during InnoREX

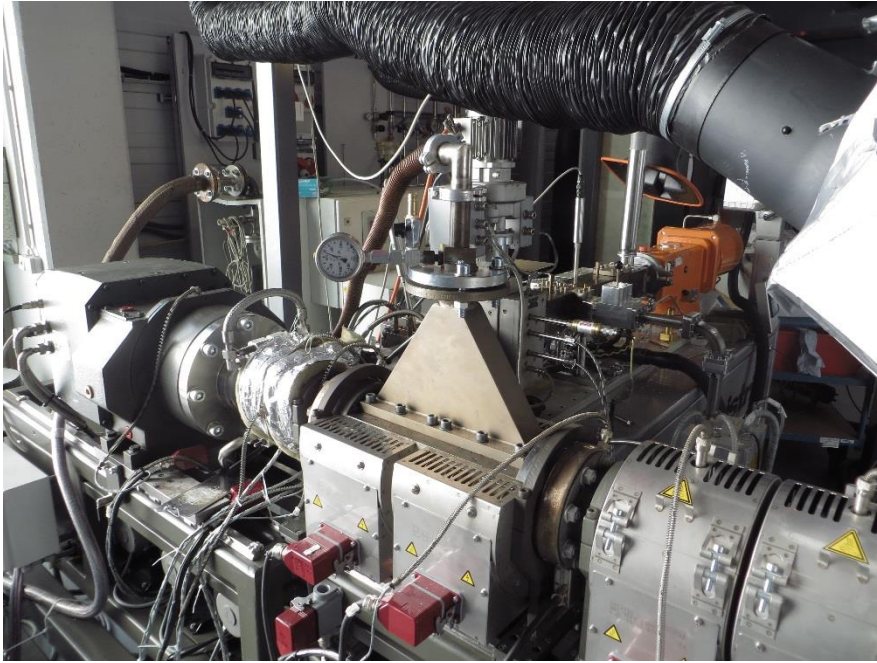


Figure 29: Melt fed MRS de-volatilization system connected to ICT twin screw extrusion system

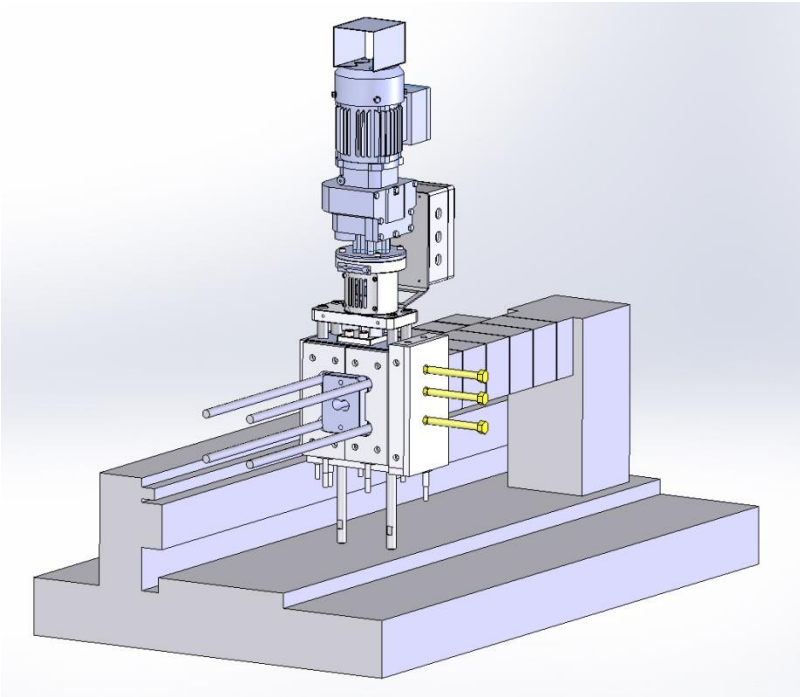


Figure 30: Schematic of extruder integrated viscosity sensing unit

Fraunhofer ICT: Project coordinator combining the InnoREX production line

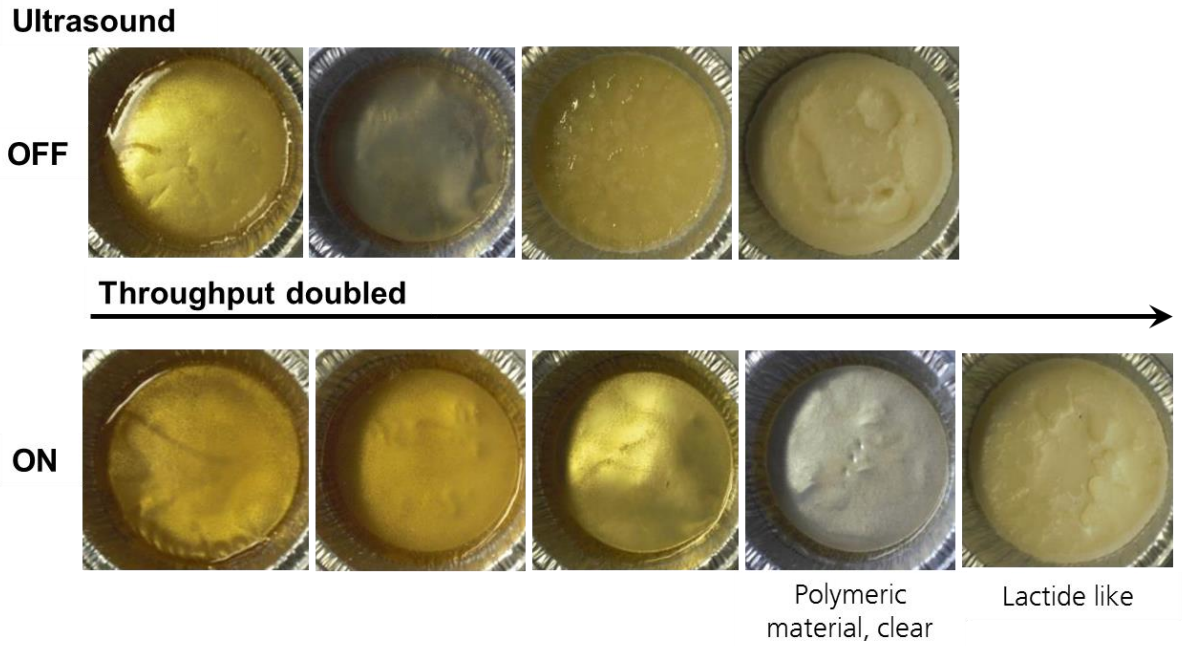


Figure 31: PLA samples produced at different settings with and without incorporated ultrasound energy

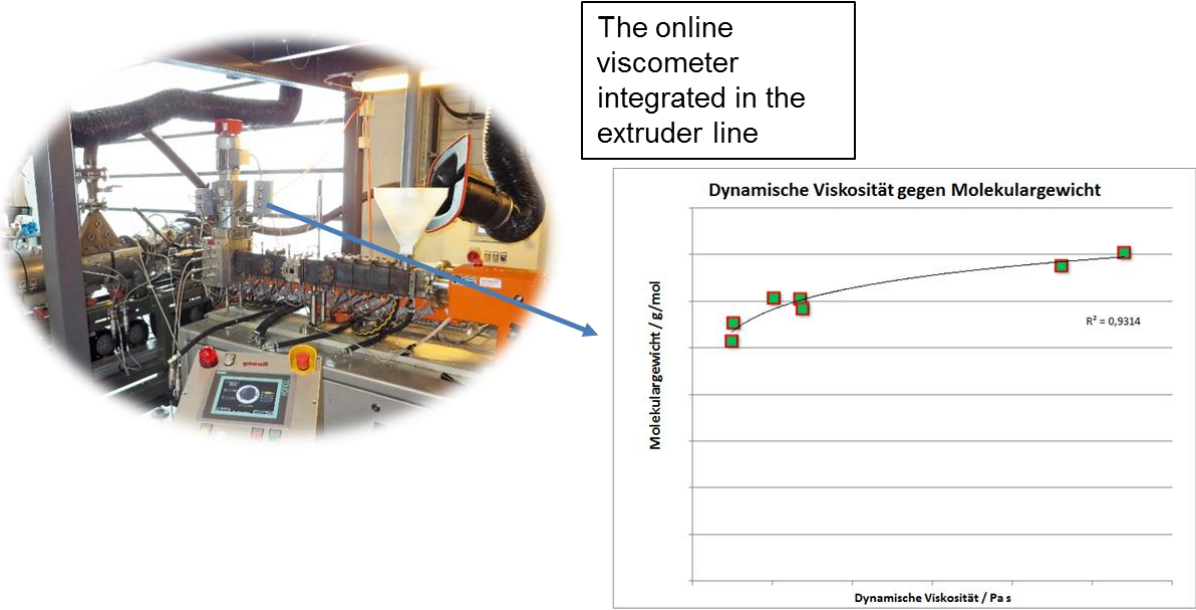


Figure 32: Online viscometer attached in processing length of twin screw and recorded dynamic viscosity with respect to molecular weight

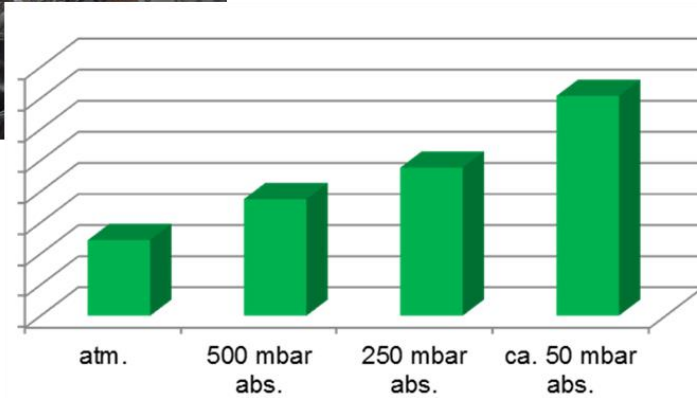
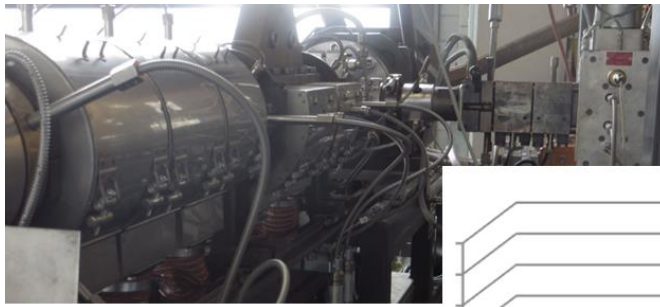


Figure 33: MRS purification extruder attached to twin screw and resulting molecular weights with varying vacuum level in MRS

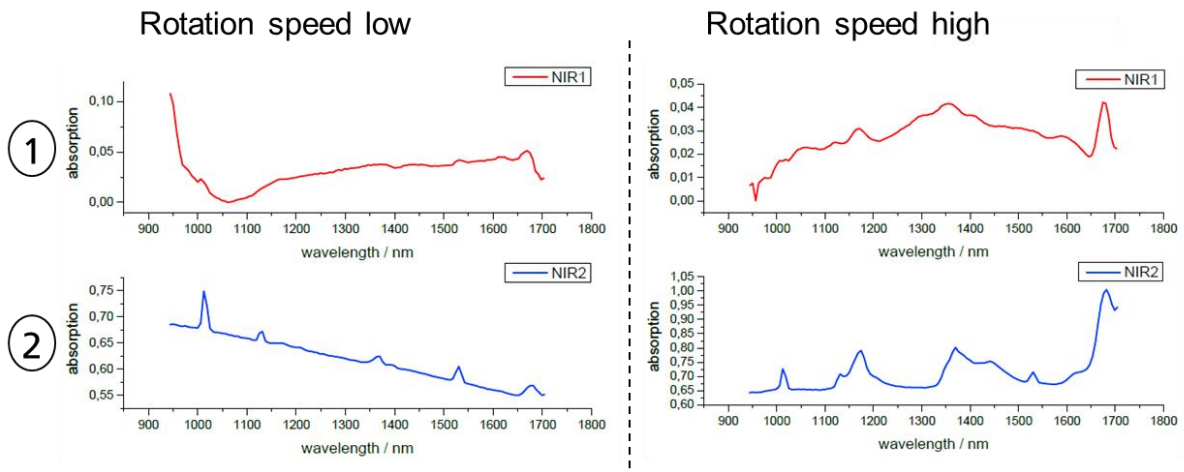
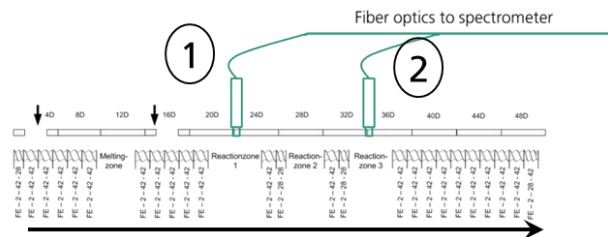
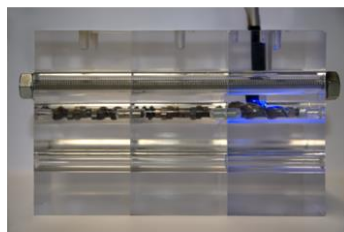


Figure 34: NIR measurement at different points within the processing length and resulting spectra with varying machine process settings

Cranfield University: Selection of simulation technique for understanding of molecular interaction and simulation of most suitable reaction mechanism:

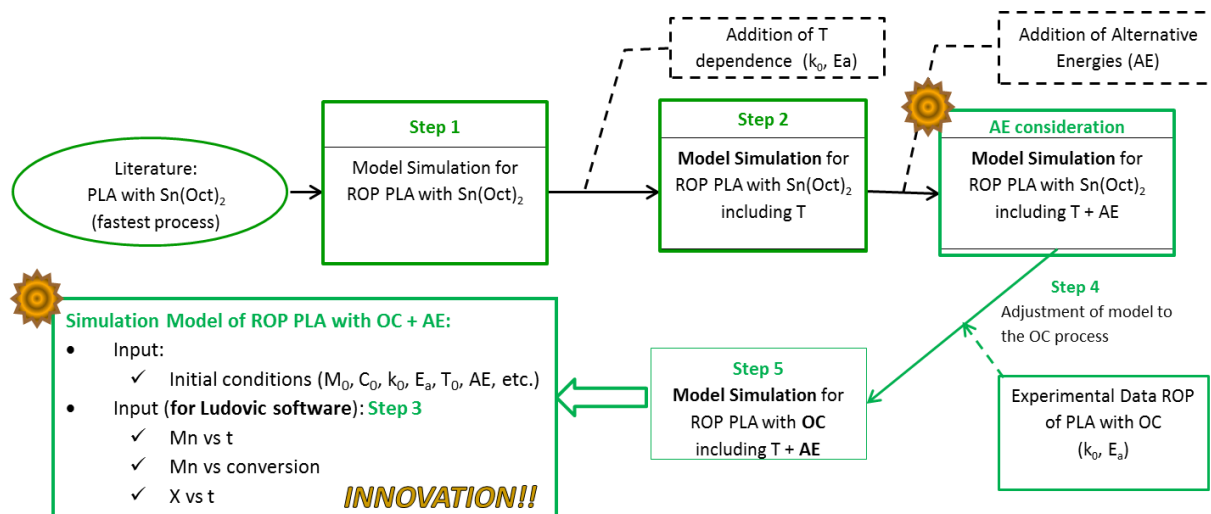


Figure 35: Project work methodology

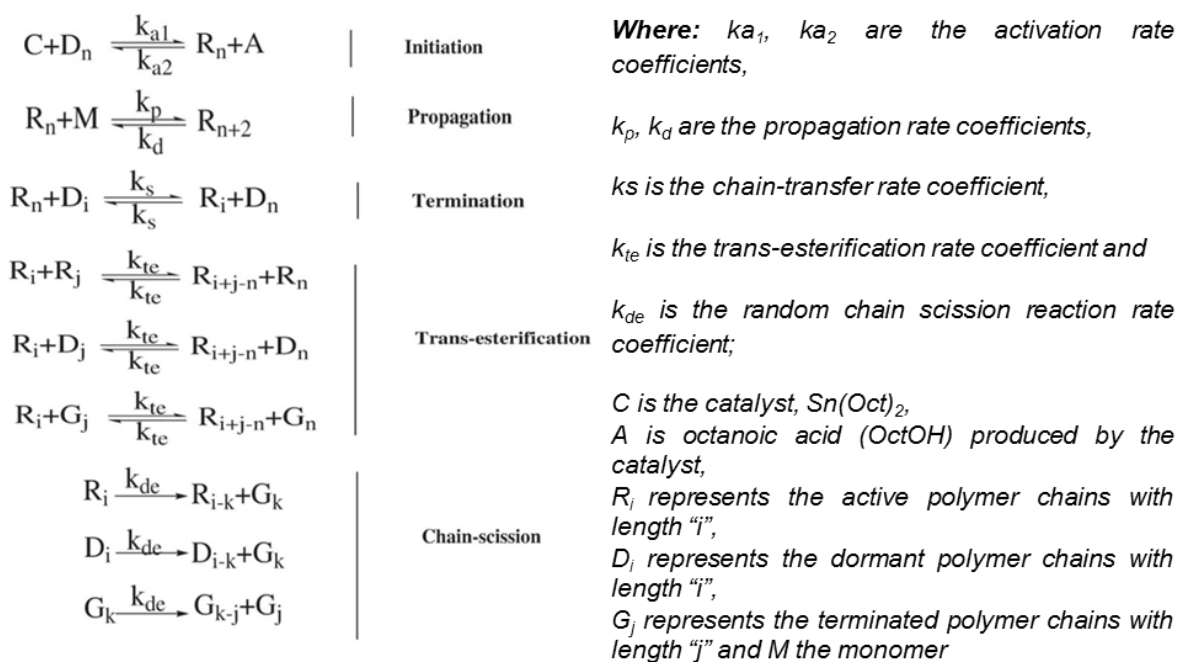


Figure 36: details of the new five stage reaction mechanism¹

¹ Yu et al. Ind. Eng. Chem. Res., vol. 50, no. 13, pp. 7927–7940, Jul. 2011

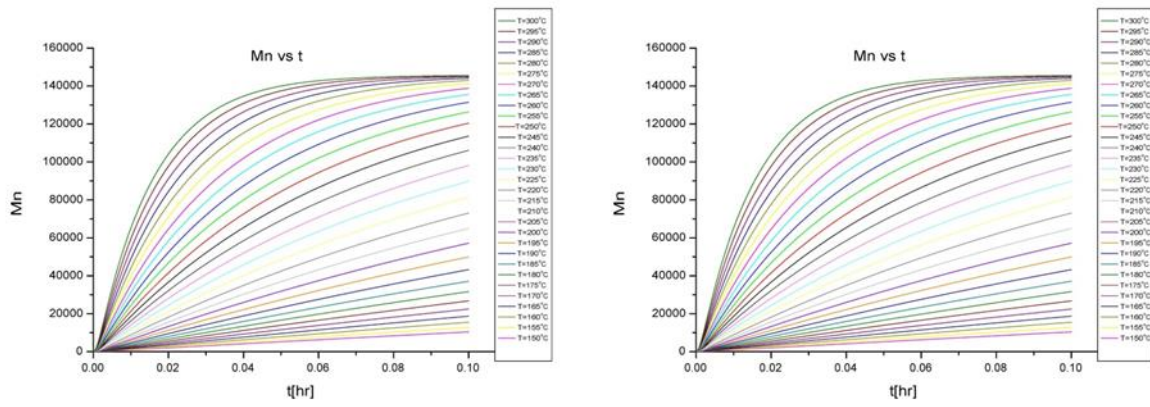


Figure 37: Isothermal curves for conversion (X) vs t and average molecular weight (\overline{M}_n) vs t

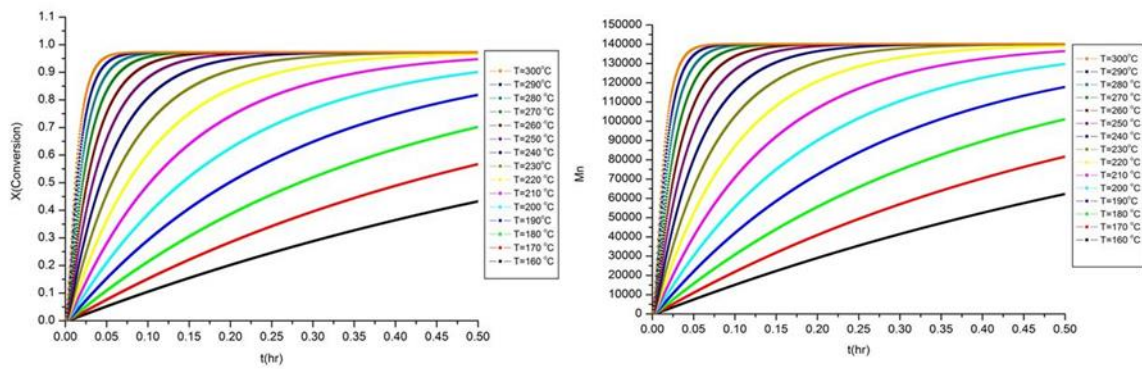


Figure 38: Isothermal curves for conversion (X) vs t and average molecular weight (\overline{M}_n) vs t

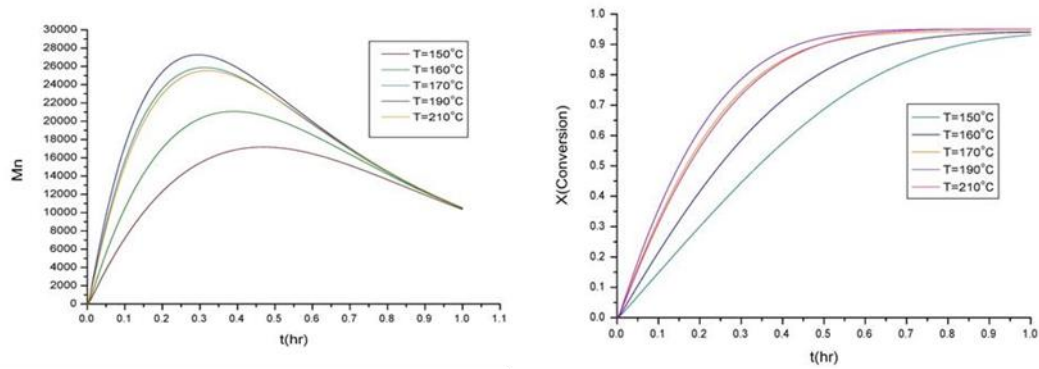


Figure 39: Isothermal curves for average molecular weight (\overline{M}_n) vs. t. and for conversion (X) vs. t.

SCC: Totally dedicated to simulation

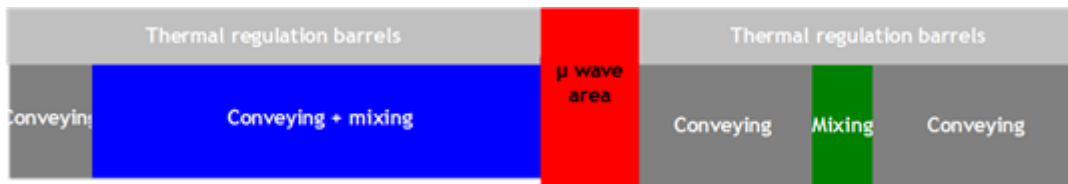


Figure 40: Screw profile with microwave device

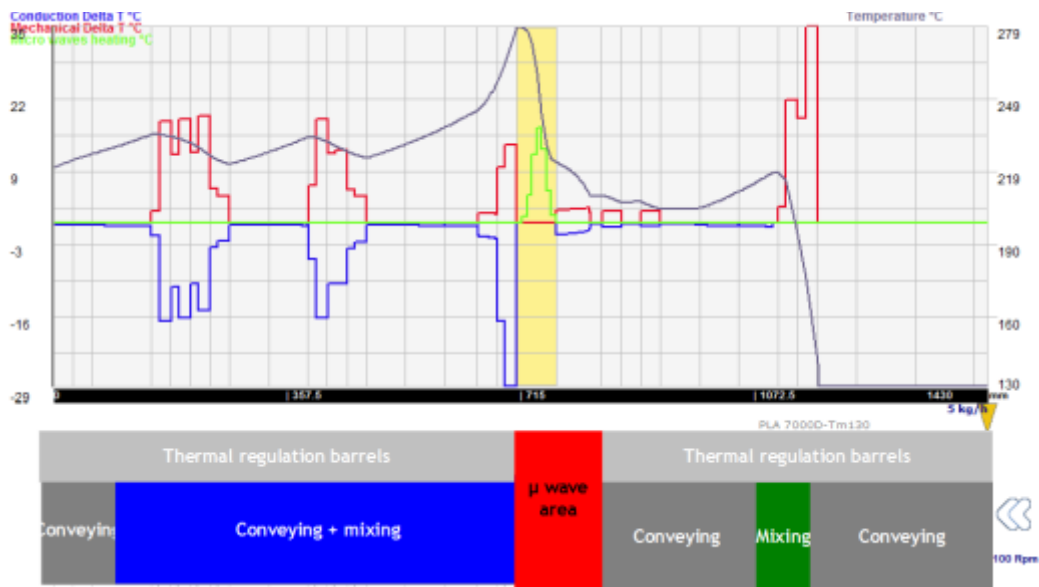


Figure 41: Temperature variation due to conduction (blue), mechanical (red) and micro-wave (100W) (green) effect and result on final temperature (grey)

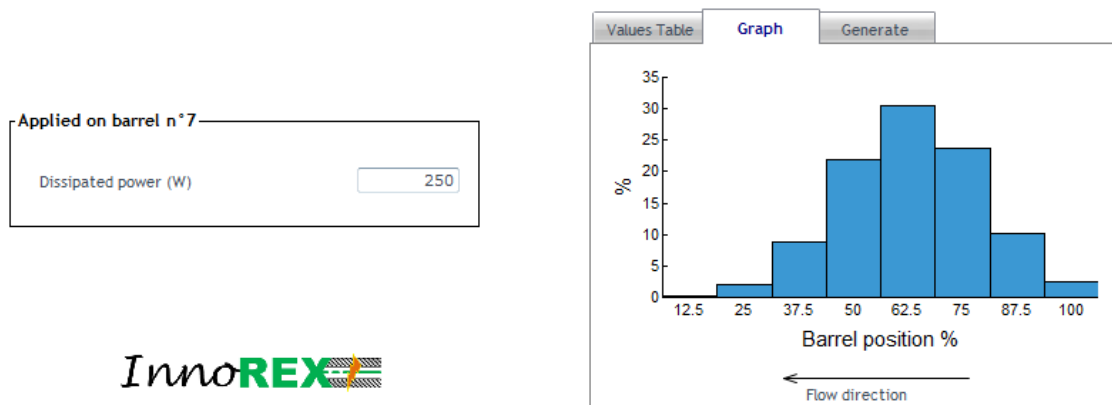


Figure 42: Microwave power Gaussian distribution

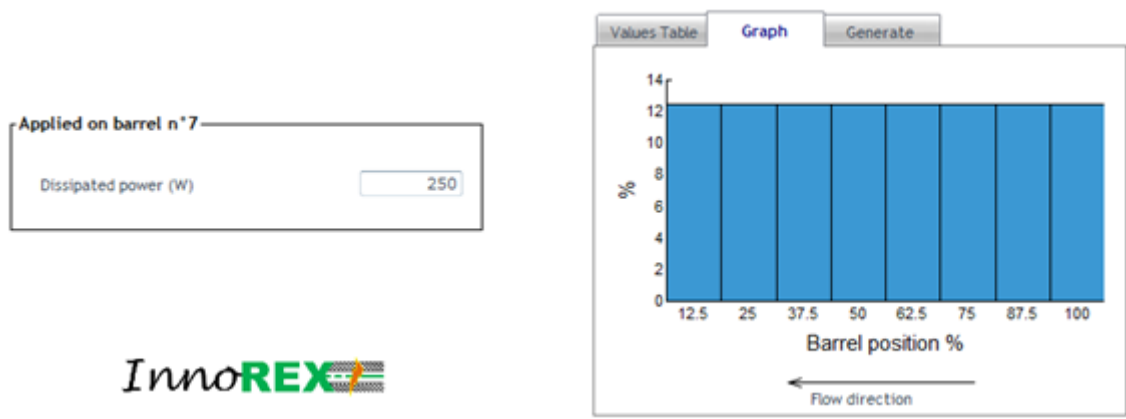


Figure 43: Microwave uniform power distribution

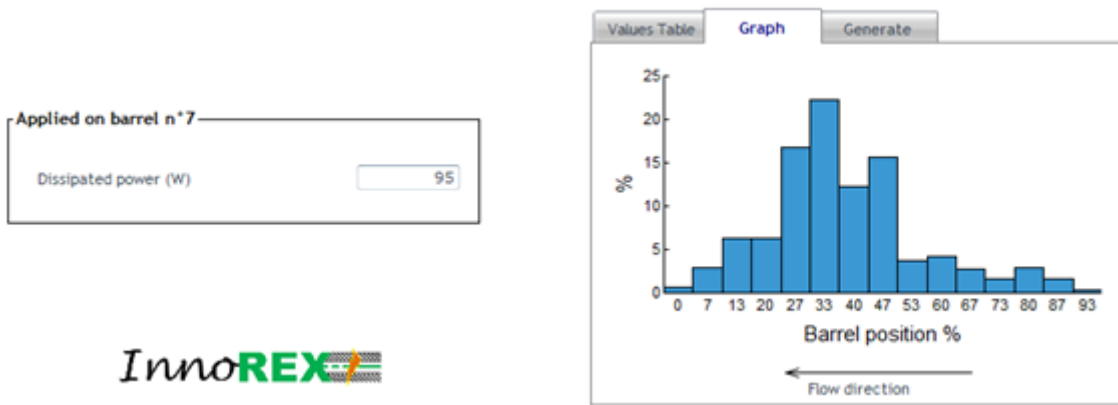


Figure 44: Microwave distribution by user defined (data from MUEGGE)

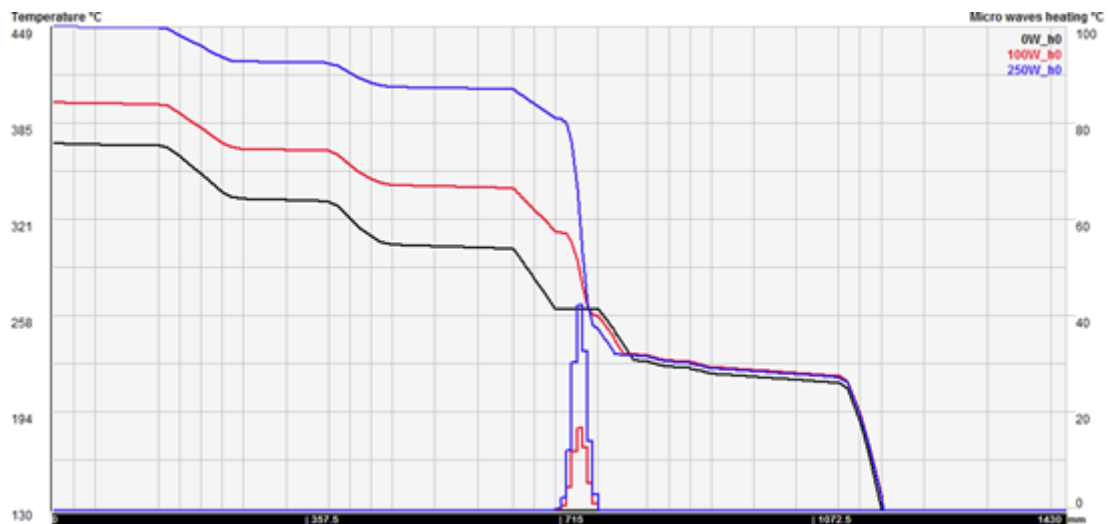


Figure 45: Effect of level of microwave power on temperature

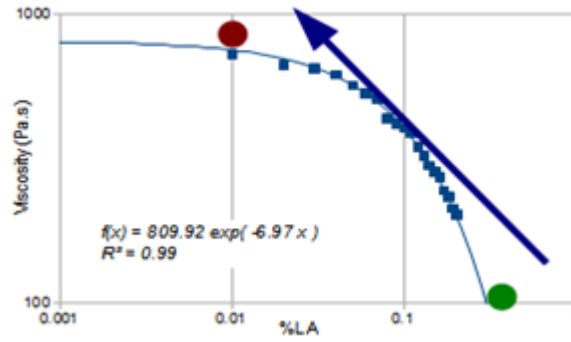


Figure 46: Evolution of viscosity as a function of %LA (curve and trend analysis)

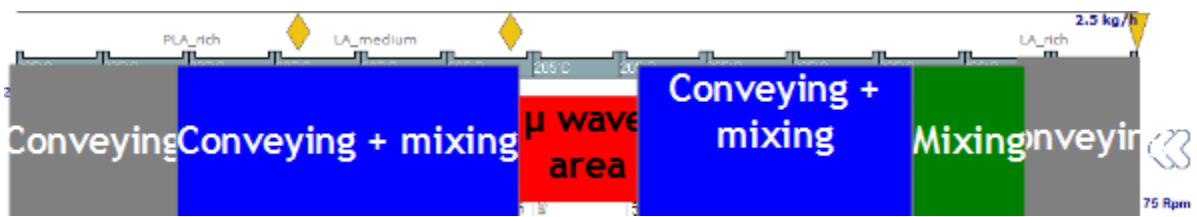


Figure 47: Ludovic® configuration with transition zones

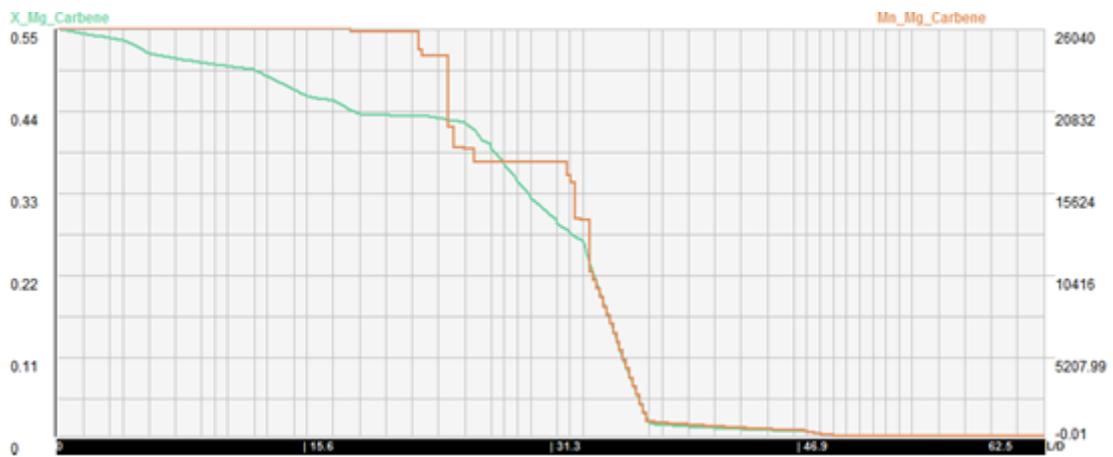


Figure 48: Simulated conversion rate and molecular weight

Materia Nova: Life Cycle Assessment (LCA) study all along the InnoREX process.

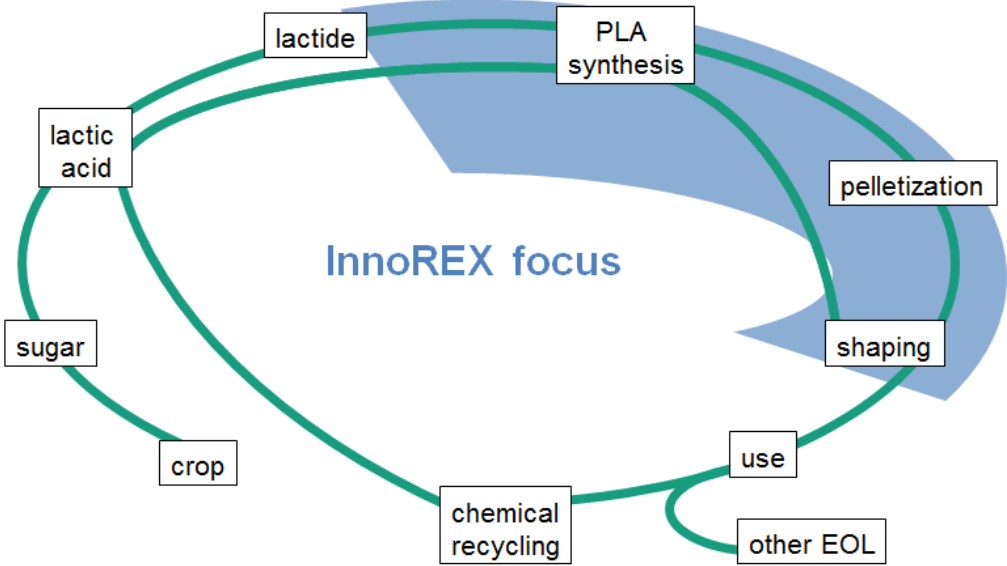


Figure 49: Highlight of the PLA life cycle steps where InnoREX innovations could provide environmental benefits

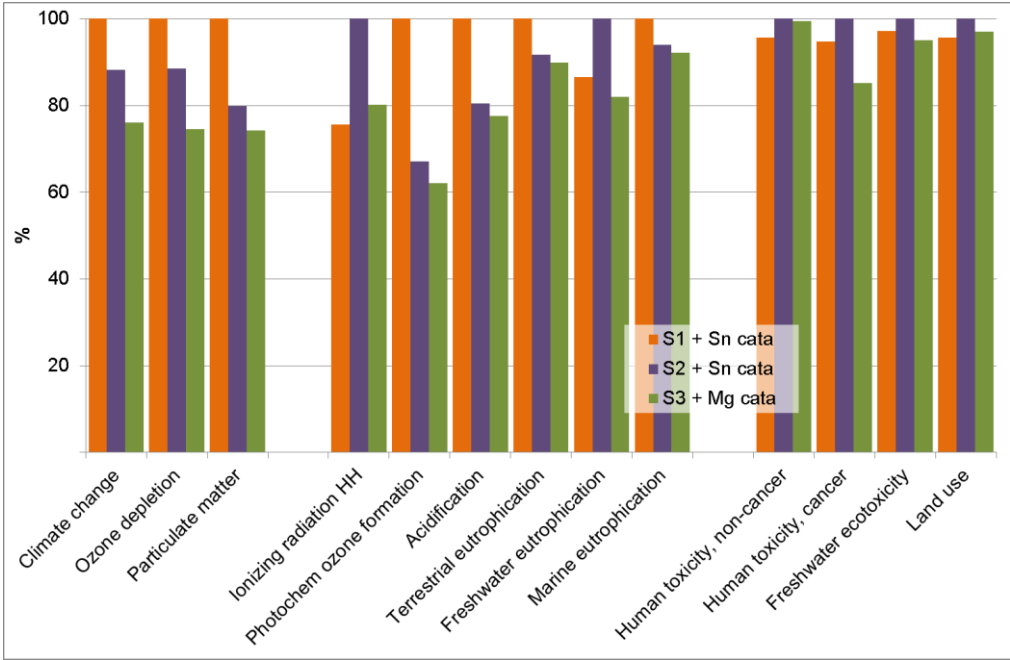


Figure 50: Compared global life cycle impacts for the three scenarios, including catalysts production and catalyst residues emissions.

AIMPLAS: Processability of new PLA grades, mainly focus on manufacturing processes: injection and extrusion.

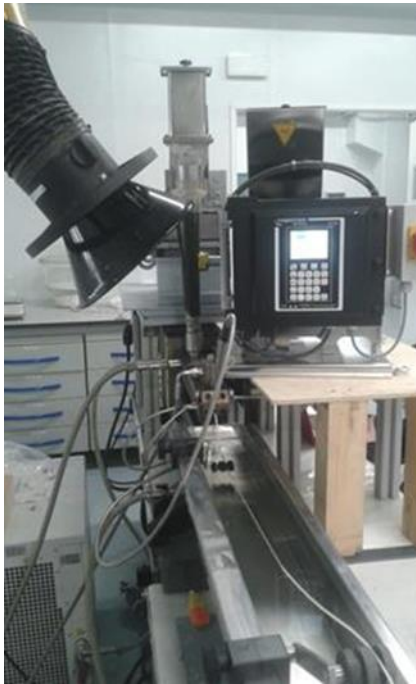


Figure 51: InnoREX PLA formulation during compounding process



Figure 52: Pure InnoREX PLA and additived PLA compound



Figure 53: Cast-sheet extrusion and test bar injection of added InnoREX PLA compound

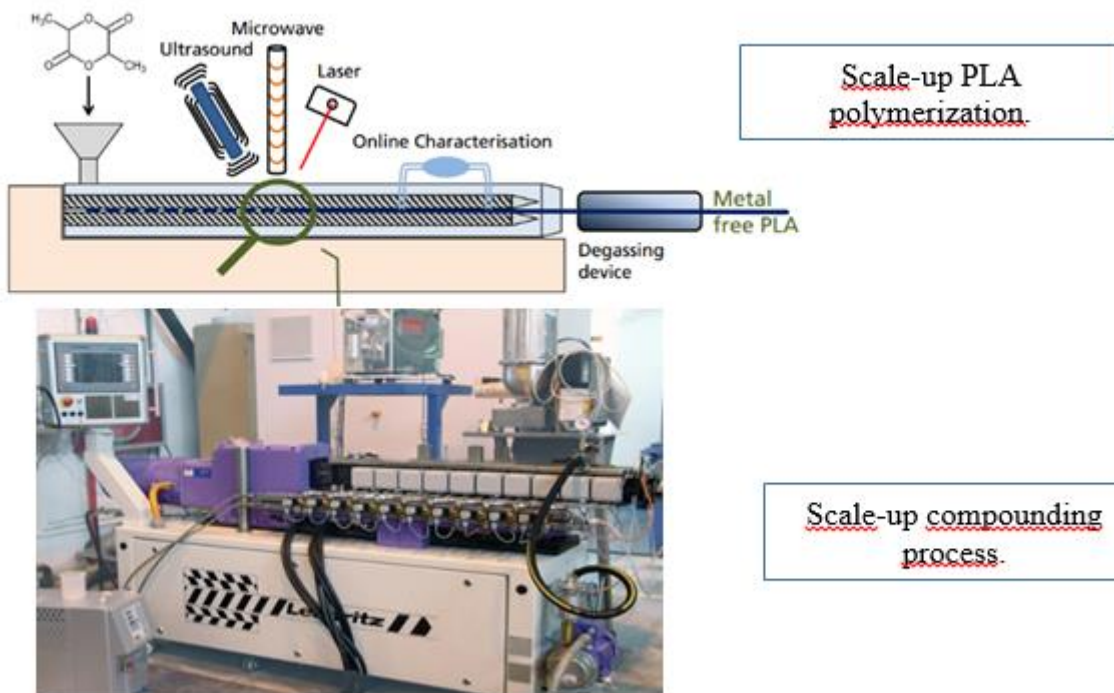


Figure 54: scale up strategy in two steps in order to study both polymerization and compounding scale up

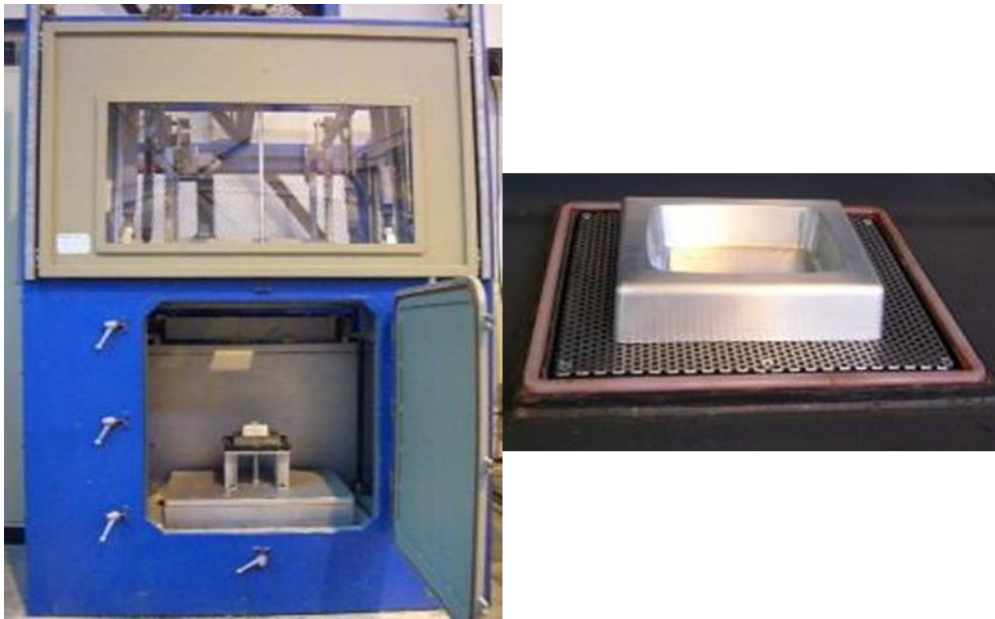


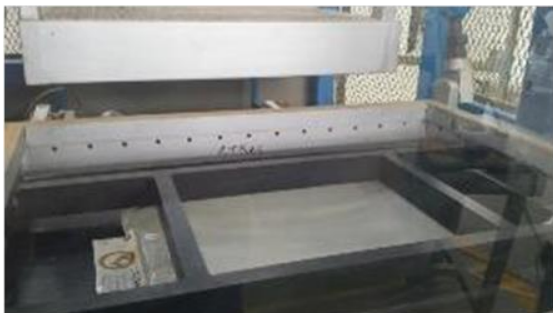
Figure 55: Thermoforming equipment and aluminum mould



Positioning the sheet in the forming area



Heating with upper and lower heaters



Soften sheet after the heating



Vacuum



Tray PLA2003D



Tray compound
PLA7001



Tray compound PLA B4

Figure 56: Steps of thermoforming process and final thermoformed trays

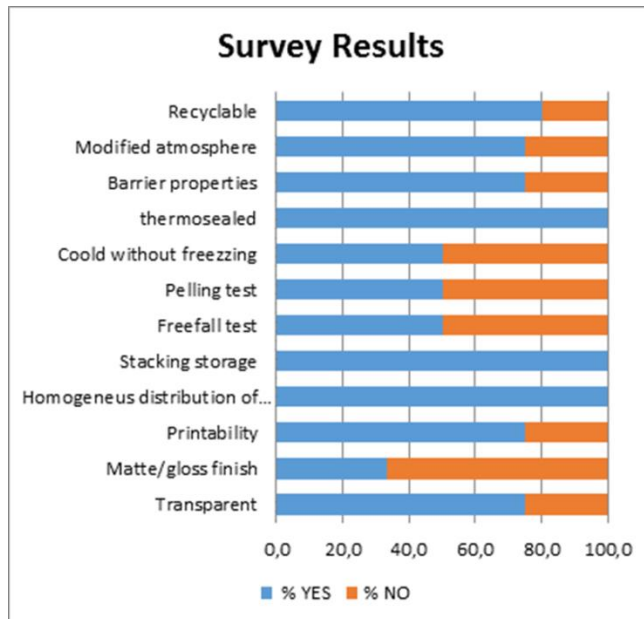


Figure 57: Results from packaging companies of the done survey by Talleres Pohuer

Talleres Pohuer: New PLA grades and case studies thereof mainly focus on manufacturing processes injection moulding.

Photos of packages from InnoREX-PLA



Figure 58: Injection moulded package from InnoREX PLA

BHI - PLA industrial up-scaling

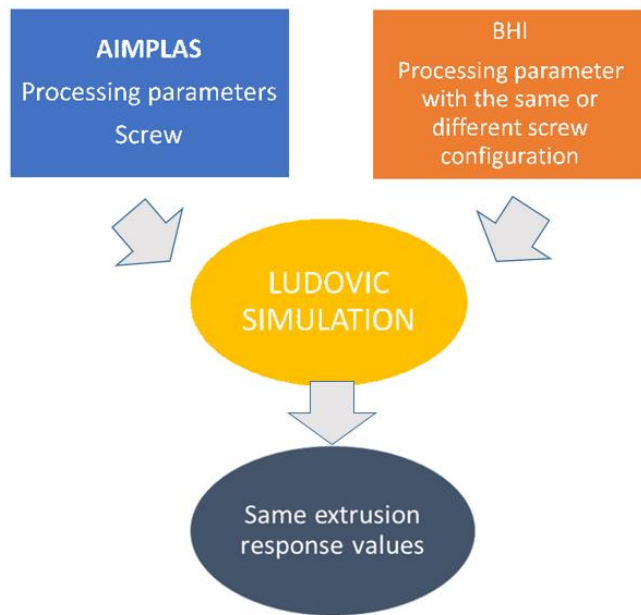


Figure 59: Work methodology of scale up step 1

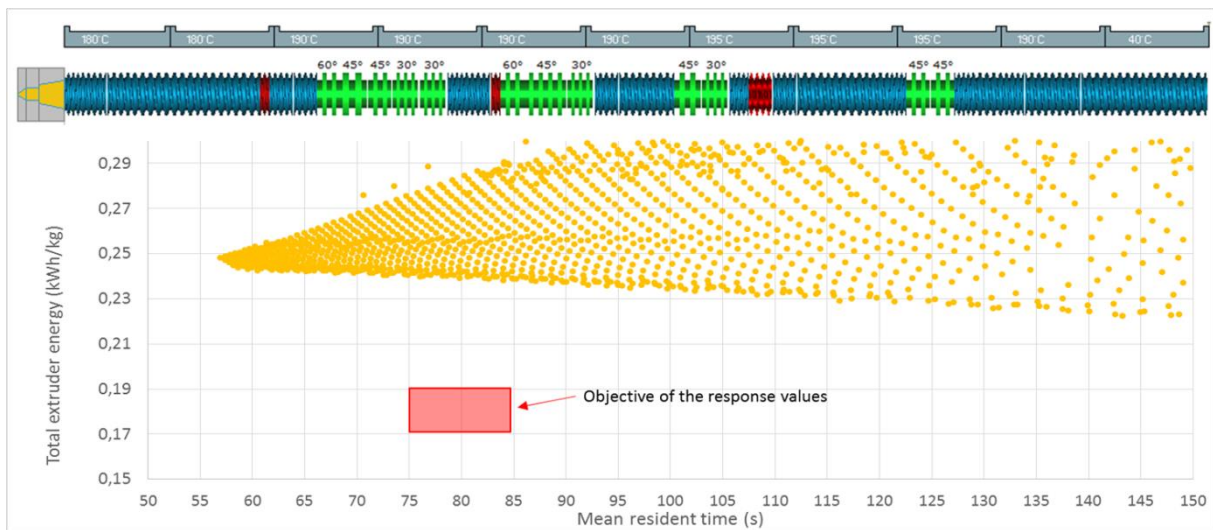


Figure 60: DOE results inputs: Flow rate (50-300kg.h), rotation speed (100-350 rpm)

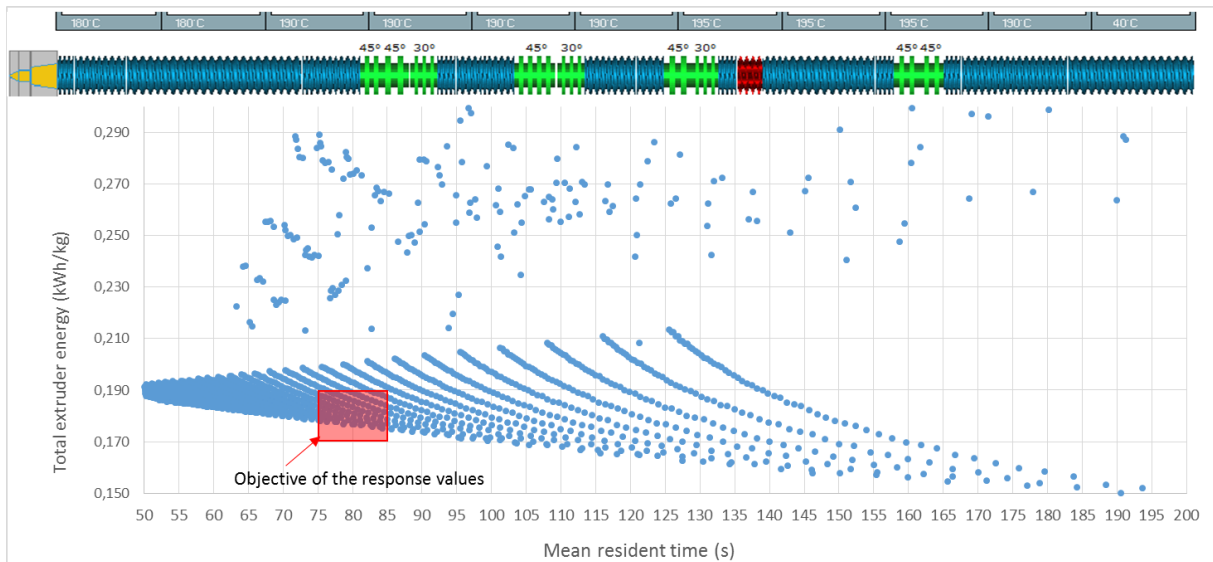


Figure 61: Scale up results with modified screw at temperatures (C) 190-180, throughput (kg/h) 140, rotation speed (rpm) 180

SAMPLE	T_m (°C)	P (bar)	Torque (N/m ₂)	Comments
PLA 2003D	186	71	3.0	OK. Thin and thick sheet.
PLA 7001D	186	76	2.8	Un-melted/gels particles
PLA 7001D	201	52	2.4	Few un-melted/gels particles
PLA 7001D + 3% chain Extender	203	126	3.5	High viscosity. Low melt strength. It is not possible to get thin sheet. Only possible thick sheet.
Mix InnoREX PLA	155	9	1.7	Very low pressure. High fluidity. It is not possible to feed constantly the die. Un-melted particles

Figure 62: Extrusion parameters of extrusion studies

Gender dimension of InnoREX project

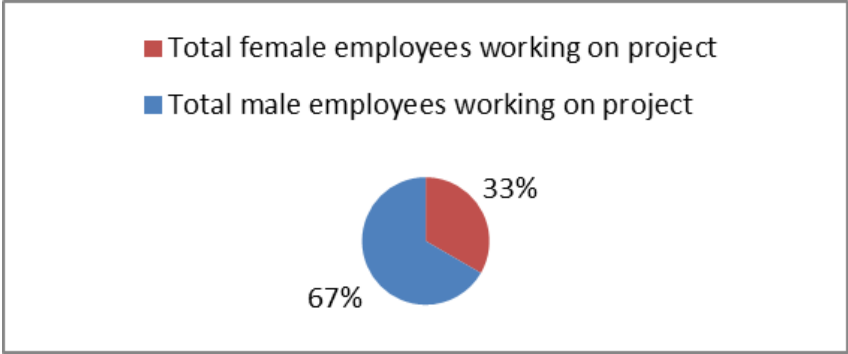


Figure 63: Overview of female and male employees in InnoREX project

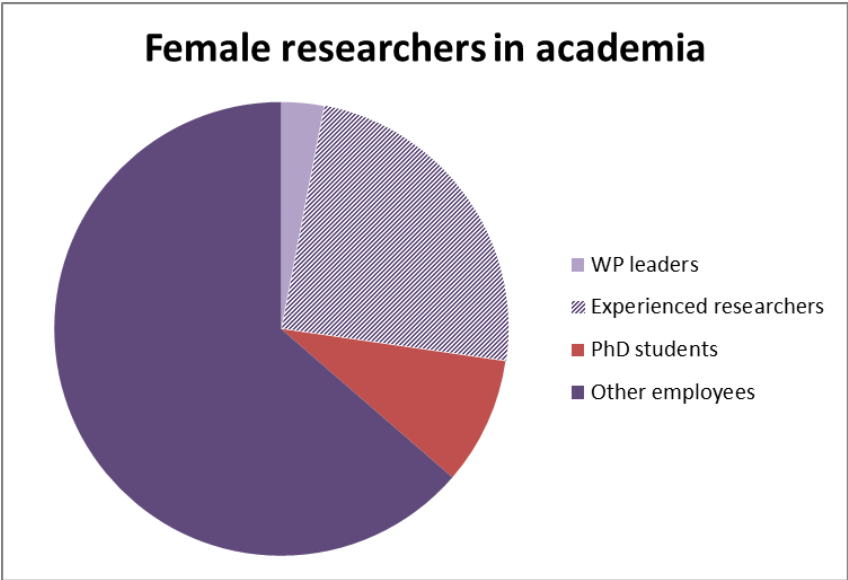


Figure 64: Distribution of female employees in academia